Int. J. Electrochem. Sci., 7 **(2012)** 9892 - 9908

International Journal of
ELECTROCHEMICAL
SCIENCE
www.electrochemsci.org

Dopamine Determination with a Biosensor Based on Catalase and Modified Carbon Paste Electrode with Zinc Oxide Nanoparticles

Koorosh Fooladsaz[1], *Masoud Negahdary*[2,*], *Ghasem Rahimi*[3], *Amir Habibi-Tamijani*[4], *Sara Parsania*[2], *Hajar Akbari-dastjerdi*[2], *Arezou Sayad*[5], *Azar Jamaleddini*[6], *Fatemeh Salahi*[6] *and Asadollah Asadi*[7]

[1] Department of Clinical Biochemistry, Zanjan University of Medical Sciences, Zanjan, Iran
[2] Department of Biology, Payame Noor University, I.R. of IRAN
[3] Department of Biology, Science and Research Branch, Islamic Azad University, Fars, Iran
[4] Department of Chemistry, Mashhad Branch, Islamic Azad University, Mashhad, Iran
[5] Department of Medical Genetics, Faculty of Medical Science, Tarbiat Modares University, Tehran, Iran
[6] Department of Chemistry, Sarvestan Branch, Islamic Azad University, Sarvestan, Iran
[7] Dept. of Biology, Faculty of Science, University of Mohaghegh Ardabili, Ardabil-Iran
[*]E-mail: masoud.negahdary@hotmail.com

Received: 31 July 2012 / *Accepted:* 7 September 2012 / *Published:* 1 October 2012

Determination level of dopamine (DA) is very important in medicine and disease diagnostic. In presented research, a biosensor designed based on catalase (CAT) and modified carbon paste electrode (CPE) with zinc oxide (ZnO) nanoparticles for Determination level of dopamine by electrochemical methods. Synthesized ZnO nanoparticles were studied by X-ray diffraction (XRD), UV-visible spectrophotometer and atomic force microscopy (AFM). Electrochemical studies were done with cyclic voltammetry (CV) and constant potential amperometry (CPA) experiments. A pair of well-defined redox peaks was observed at the CAT / ZnO Nps/ CPE with The formal potential (E^o) equal to + (92.5 ± 1) mV. Zinc oxide nanoparticles could play a key role in creates the CAT CV response and facile electron transfer between CAT and CPE. The CAT / ZnO Nps/ CPE showed a good sensitive state towards oxidation of DA. The designed biosensor showed a good stability and retains its 91% activity after 21 days.

Keywords: Dopamine biosensor, catalase, zinc oxide nanoparticles, bioelectrochemistry

1. INTRODUCTION

A biosensor is a chemical sensing device in which a biologically derived recognition entity is coupled to a transducer, to allow the quantitative development of some complex biochemical parameter, and in other word a biosensor is an analytical device incorporating a deliberate and intimate combination of a specific biological element (that creates a recognition event) and a physical element (that transduces the recognition event) [1-3]. Biosensors can have a variety of biomedical, industry, and military applications [4-5]. Biosensors can be grouped according to their biological element or their transduction element [6-7]. Biological elements include enzymes, antibodies, micro-organisms, biological tissue, and organelles [8]. The method of transduction depends on the type of physicochemical change resulting from the sensing event. Measurement of analyte concentrations is essential in the diagnosis and treatment of diseases and in many other areas of chemical and biological research [9-11]. In this research analyte was dopamine. Nanoscience and nanotechnology involve studying and working with matter on an ultra-small scale (1×10^{-9} m). One nanometer is one-millionth of a millimeter and a single human hair is around 80,000 nanometers in width. Nanoscience and nanotechnology have a many applications in other sciences such as medicine, physics, engineering, biology, chemistry and etc. [12-14]. The revolution of nanotechnology in molecular biology gives an opportunity to detect and manipulate atoms and molecules at the molecular and cellular level [15-16]. Nanoparticles have numerous possible applications in biosensors. For example, functional nanoparticles (electronic, optical and magnetic) bound to biological molecules (e.g. peptides, proteins, nucleic acids) have been developed for use in biosensors to detect and amplify various signals [17]. Some of the nanoparticle-based sensors are include the acoustic wave biosensors, optical biosensors, magnetic and electrochemical biosensors. Metal nanoparticles (Nps) can be used to enhance the amount of immobilized biomolecules in construction of a sensor [18-19]. Metal nanoparticles have been used to catalyze biochemical reactions and this capability can be usefully employed in biosensor design. Among oxide nanoparticles, ZnO nanostructure material has gained much interest owing to its wide applications for various devices such as solar cells, transducers, transparent conducting electrodes, sensors, and catalysts [20-23]. In this research we used of zinc oxide nanoparticles as facile electron transfer. Enzymes are proteins with high catalytic activity and selectivity towards substrates. Their commercial availability at high purity levels makes them very attractive for mass production of enzyme sensors [24-25]. Their main limitations are that pH, ionic strength, chemical inhibitors, and temperature affect their activity [26]. Most enzymes lose their activity when exposed to temperatures above 60^{o}C. Catalase (CAT) is a common enzyme present in most all living organisms and a very potent catalyst [27]. Catalase is found in the blood, plant cells, animal cells, and other living organisms. Catalase converts the harmful byproduct of metabolism, Hydrogen Peroxide, into water and oxygen [28-29]. This enzyme is a tetramer of four polypeptide chains, each over 500 amino acids long. It contains four porphyrin heme (iron) groups which allow the enzyme to react with the hydrogen peroxide [30]. The optimum pH for catalase is approximately neutral (pH 7.0). In presented research we used of catalase in oxidation and reduction reactions. The described biosensor in this research designed for detect dopamine. You can see molecular structure of dopamine in figure 1.

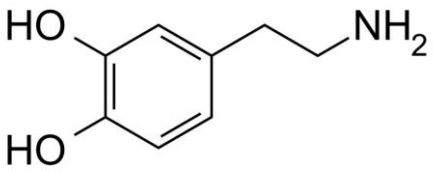

Figure 1. Molecular structure of dopamine

Dopamine (3, 4 dihydroxyphenylethylamine, DAH_2) is an important brain neurotransmitter molecule of catecholamine and its deficiency leads to brain disorders such Parkinsonism, where dopamine (DA) levels are reduced and schizophrenia, which can be related to excess activity of dopamine [31-34]. It used by neurons in several brain regions involved in motivation and reinforcement, most importantly the nucleus accumbens. Electrochemical behavior of dopamine plays important roles in its physiological functions, and is a key factor in diagnosis of some diseases in clinical medicine. Hence, it is desirable to develop an electrochemical method to study electron transfer processes [35-38]. Here important aim of this research was introduce a new method for determination of dopamine in micro molar ranges.

2. EXPERIMENTAL

2.1. Materials

Dopamine purchased from Fluka Chemical Co (USA), and used without further purification. Catalase, zinc nitrate ($Zn(NO_3)_2 \cdot 4H_2O$) and sodium hydroxide (NaOH) were purchased from Sigma-Aldrich. Other Reagents purchased from Merck. The supporting electrolyte used for all experiments was 0.1 M pH 7 phosphate buffer solution (PBS), which prepared by using a potassium phosphate solution (KH_2PO_4 and K_2HPO_4 from Merck; 0.1 M total phosphate) at pH 7.0. All the reagents used were of analytical grade and all aqueous solutions were prepared using doubly distilled water generated by a Barnstead water system.

2.2. Apparatus

Cyclic voltammetry (CV) and constant potential amperometry (CPA) experiments were performed using an Autolab potentiostat PGSTAT 302 (Eco Chemie, Utrecht, The Netherlands) driven by the General purpose Electrochemical systems data processing software (GPES, software version 4.9, Eco Chemie). A conventional three-electrode cell was employed throughout the experiments, with bare or ZnO nanoparticles modified carbon paste electrode (4.0mm diameter) as a working electrode, a saturated calomel electrode (SCE) as a reference electrode, and a platinum electrode as a counter electrode. Surface morphological studies of ZnO nanoparticles were performed by using a DME atomic force microscope (AFM) with a Dual Scope C-21 controller and DS 95-50 scanner. The phase characterization of ZnO nanoparticles was performed by means of X-ray diffraction (XRD) using a

D/Max-RA diffractometer with CuKα radiation. The absorbance properties of prepared nanoparticles were measured and recorded by using a TU-1901 double-beam UV-visible spectrophotometer. The experimental solutions were de-aerated using highly pure nitrogen for 30 min. and a nitrogen atmosphere was kept over the solutions during the measurements. All the electrochemical measurements were carried out in 0.1 M PBS, pH 7.0 at 25 ± 1 ^{o}C.

2.3. Preparation of ZnO nanoparticles

To prepare of ZnO NPs, in a typical experiment, a 0.45M aqueous solution of zinc nitrate (Zn $(NO_3)_2{\cdot}4H_2O$) and 0.9M aqueous solution of sodium hydroxide (NaOH) were prepared in distilled water. Then, the beaker containing NaOH solution was heated at the temperature of about 55°C. The Zn $(NO_3)_2$ solution was added drop wise (slowly for 1 h) to the above-heated solution under high-speed stirring. The beaker was sealed at this condition for 2 hours. The precipitated ZnO NPs were cleaned with deionized water and ethanol then dried in air atmosphere at about 60°C.

2.4. Preparation of bare carbon paste electrode

The carbon powder (particle size 50 mm, density 20-30g/100mL) was mixed with the binder, silicone oil, in an agate mortar and homogenized using the pestle. The electrode consisted of a Teflon well, mounted at the end of a Teflon tube. The prepared paste was filled into the Teflon well. A copper wire fixed to a graphite rod and inserted into the Teflon tube served to establish electrical contact with the external circuit. The electrode surface of the working electrode was renewed mechanically by smoothing some paste off and then polishing on a piece of transparent paper before conducting each of the experiments. The experiments were performed in unstirred solutions.

2.5. Preparation of ZnO *nanoparticles modified carbon paste electrode*

The ZnO nanoparticles modified carbon paste electrode was prepared by hand mixing of carbon powder, binder and 10 mg ZnO nanoparticle with silicon oil in an agate mortar to produce a homogenous carbon paste. Other steps of produced modified carbon paste electrode were similar to preparation of bare carbon paste electrode. A conventional three electrode cell was employed throughout the experiments, with bare or ZnO nanoparticles modified carbon paste electrode (4.0 mm diameter) as a working electrode, an saturated calomel electrode (SCE) as a reference electrode and a platinum electrode as a counter electrode.

2.6. Preparation of CAT- ZnO *nanoparticles modified carbon paste electrode*

The modified electrode that produced in previous section was used for production of CAT - ZnO nanoparticles modified carbon paste electrode. In this section, the CAT was immobilized by dropping 3 µl of 10 mg/ml of the enzyme solution onto the ZnO nanoparticles modified carbon paste

electrode and dried for about 30 min at room temperature. The electrode was then gently washed with de-ionized double distilled water and put at 4 ºC when not in use.

3. RESULTS AND DISCUSSION

3.1. UV-visible spectroscopy of Zno nanoparticles

UV-visible spectroscopy is one of the most widely used techniques for structural characterization of metal nanoparticles [39]. These nanoparticles exhibit a strong UV-vis absorption band that is not present in the spectrum of the bulk metal [40]. The UV-VIS spectral range is approximately 190 to 900 nm, as defined by the working range of typical commercial UV-VIS spectrophotometers. The UV–visible absorption spectra of ZnO nanoparticles are shown in Figure 2 although the wavelength of our spectrometer is limited by the light source, the absorption band of the ZnO nanoparticles have been shows a blue shift (from 275 nm to 350 nm) due to the quantum confinement of the excitons present in the sample compare with bulk ZnO particles. This optical phenomenon indicates that these nanoparticles show the quantum size effect [41].

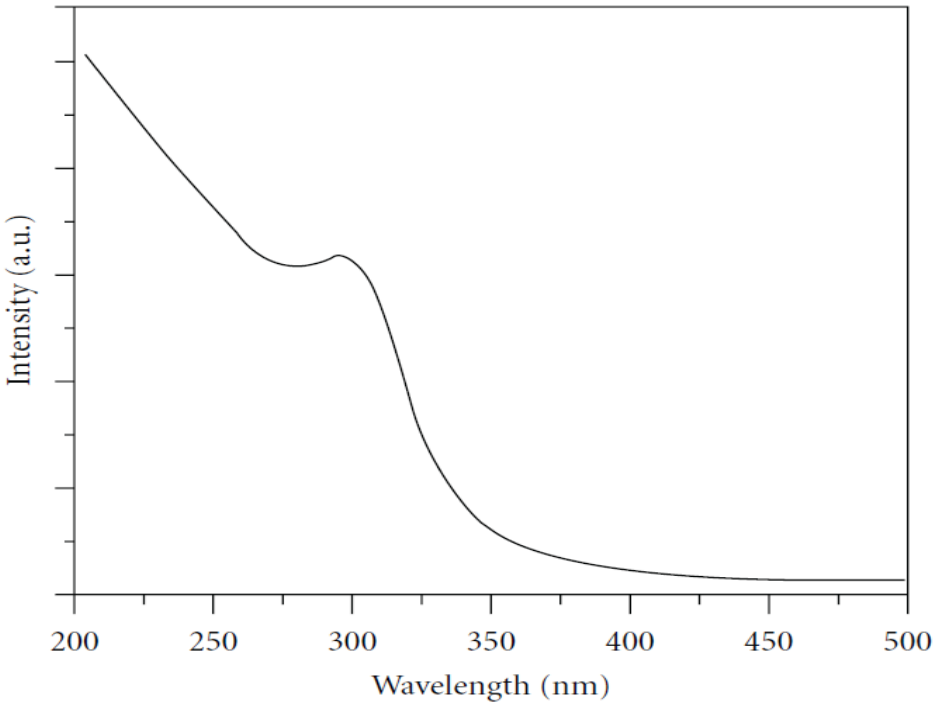

Figure 2. UV–visible absorption spectra of ZnO nanoparticles

3.2. X-Ray diffraction of Zno nanoparticles

The x-ray diffraction data were recorded by using Cu Kα radiation (1.5406 A^o). The intensity data were collected over a 2θ range of 20-80^o. The average grain size of the samples was estimated

with the help of Scherrer equation using the diffraction intensity of (101) peak. x-ray diffraction studies confirmed that the synthesized materials were ZnO with wurtzite phase and all the diffraction peaks agreed with the reported JCPDS data and no characteristic peaks were observed other than ZnO. The mean grain size of the particles was determined from the XRD line broadening measurement using Scherrer equation[42]:

$$D=0.89\lambda / (\beta Cos\theta) \quad (1)$$

Where λ is the wavelength (Cu Kα), β is the full width at the half- maximum (FWHM) of the ZnO (101) line and θ is the diffraction angle. A definite line broadening of the diffraction peaks is an indication that the synthesized materials are in nanometer range. The lattice parameters calculated were also in agreement with the reported values. The reaction temperature greatly influences the particle morphology of as-prepared ZnO powders. Figure 3 (a&b) shows the XRD patterns of ZnO nanoparticles.

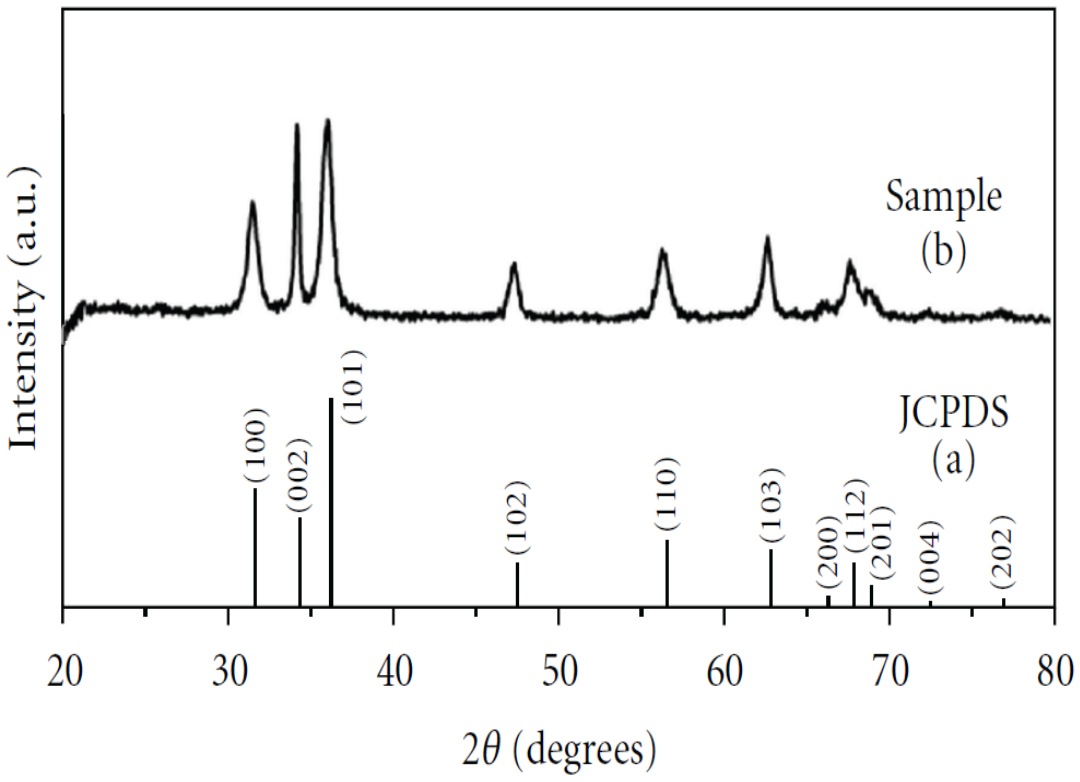

Figure 3. XRD patterns of ZnO nanoparticles

3.3. Microscopic Investigation of ZnO Nanoparticles

As it is well known, the properties of a broad range of materials and the performance of a large variety of devices depend strongly on their surface characteristics [43]. For the structure investigation of ZnO nanoparticles the utilization of atomic force microscopy (AFM) was considered. Figure 4.A–C

depict the AFM images of the bare carbon paste electrode and modified carbon paste electrode with ZnO nanoparticles; figure 4 A, depict the AFM images of the bare carbon paste electrode; figure 4 B, depict the AFM images of the modified carbon paste electrode with ZnO nanoparticles, in this part It can be seen that small particles with average size of less than 30 nm is almost uniformly distributed on the surface of carbon paste electrode; These modified carbon paste electrode can present a significant effect for the better immobilization of catalase enzyme on their surfaces; and figure 4 C, depict the 3D AFM images of the modified carbon paste electrode with ZnO nanoparticles.

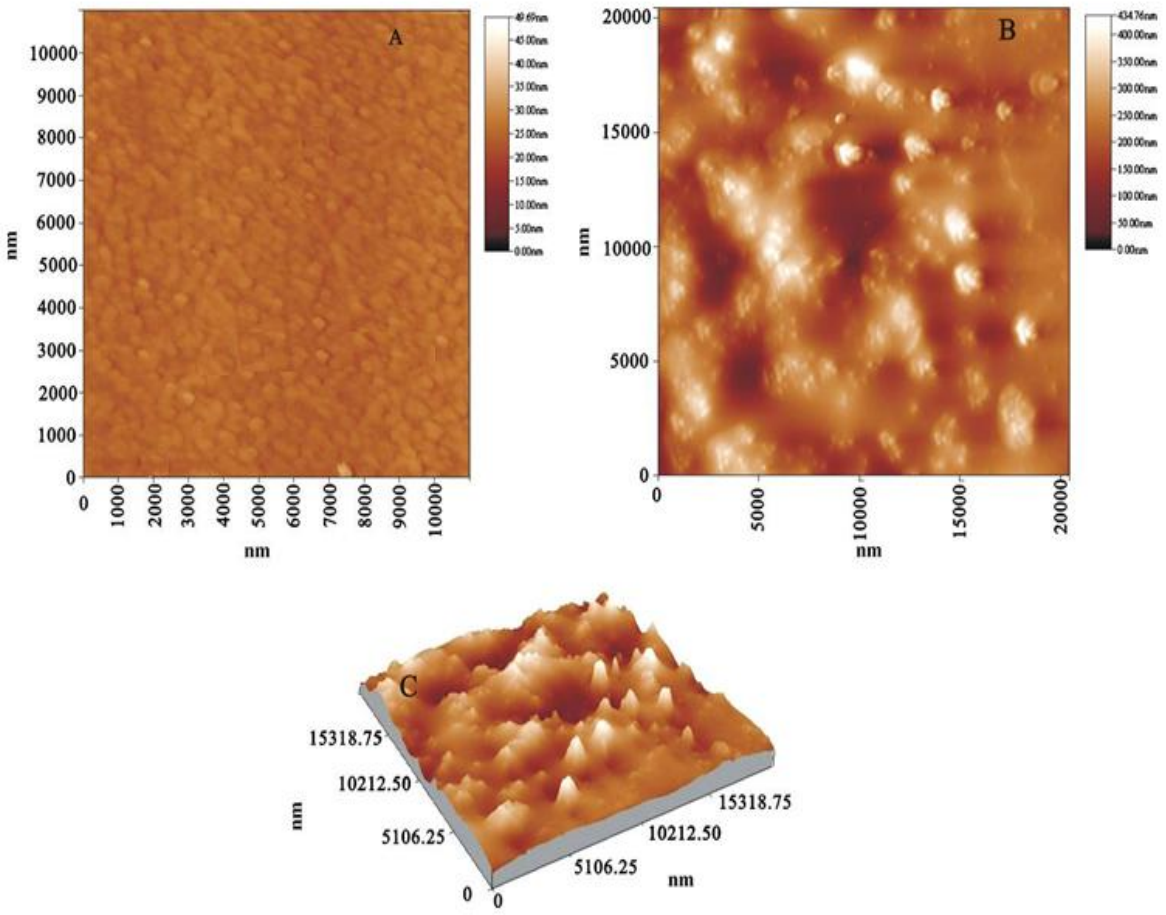

Figure 4. AFM images of bare carbon paste electrode(A); modified carbon paste electrode with ZnO nanoparticles(B) and 3D images of the modified carbon paste electrode with ZnO nanoparticles(C).

3.4. Direct electrochemistry of catalase immobilized on modified carbon paste electrode with ZnO nanoparticles

The direct electrochemistry behavior of CAT / ZnO Nps/ CPE was studied as shown in Figure 5(a&b). It can be seen in cyclic voltammograms (Figure 5(b)) that a pair of well-defined redox peaks was observed at the CAT / ZnO Nps/ CPE in a 0.1 mol L^{-1} phosphate buffer solution (PBS) of pH 7.0 at a scan rate of 100mVs^{-1} compared to the ZnO Nps/ CPE (Figure 5(a)). Its anodic peak potential and

cathodic peak potential were located at +275mV and −90mV (vs. SCE), respectively. The peak-to-peak separation (ΔE) was calculated about 185 mV. Obviously, these peaks were attributed to the redox reaction of the electroactive probe of catalase. CAT / CPE also showed the response of catalase, but the response was much smaller than that of CAT / ZnO Nps/ CPE (not shown here). Thus, the adsorption of catalase and ZnO nanoparticles on electrode surface played an important role in facilitating the electron exchange between the electroactive center of catalase and CPE. The formal potential (E^o) of catalase, estimated as the midpoint of reduction and oxidation potentials, was + (92.5 ± 1) mV. In a research, Karimi-Shervedani and Alinajafi-Najafabadi worked on electrochemical determination of dopamine on a glassy carbon electrode Modified by using nanostructure ruthenium oxide hexacyanoferrate/ruthenium hexacyanoferrate thin film and E^o for them work calculated about +313 mV [44]. In other research Manjunatha et al worked on cyclic voltammetric studies of dopamine at lamotrigine and TX-100 modified carbon paste electrode and E^o for them work calculated about +201 mV[45].

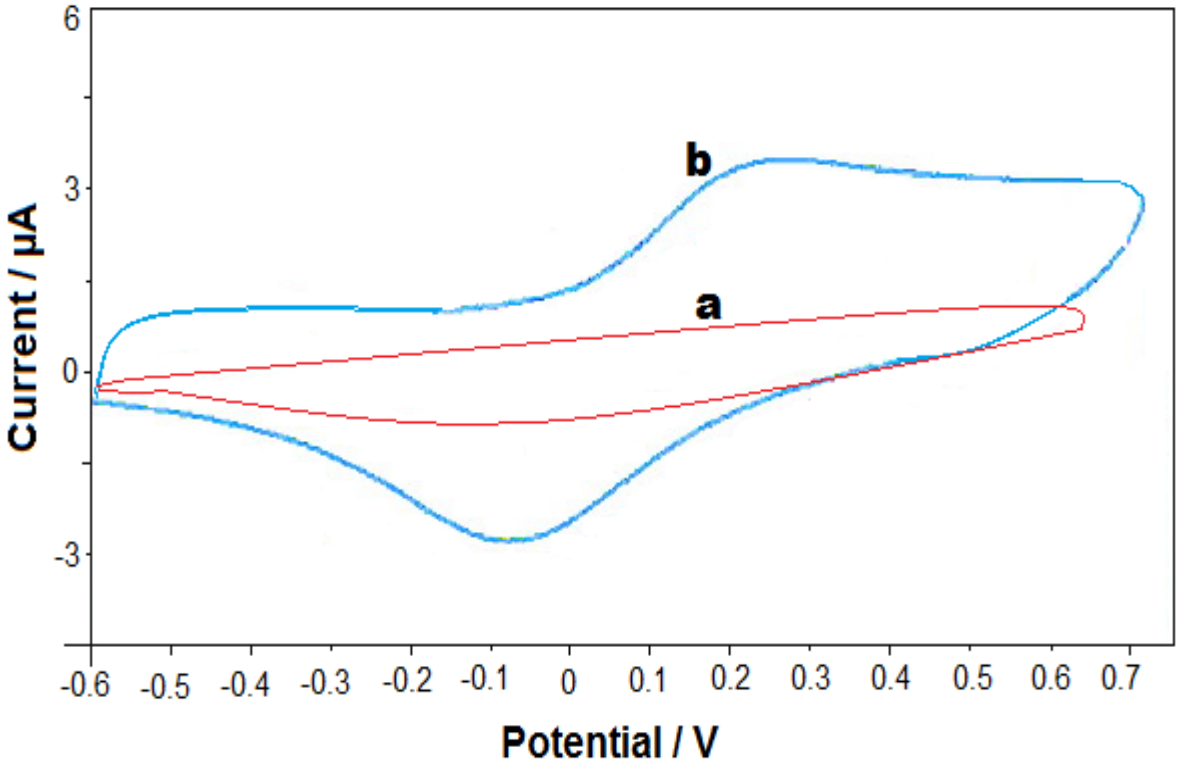

Figure 5. Cyclic voltammograms of (a) bare CPE and (b) CAT / ZnO Nps/ CPE in (0.1 M PBS with pH 7.0 and scan rate. 100 mV/s).

The collected voltammogram (CV) in Figure 6(a) substantiated a statement that the nanometer-scale of Zinc oxide nanoparticles could play a key role in creates the catalase CV response. On the grounds that the surface-to-volume ratio increases with the size decrease in nanoparticles and because due to this fact that the protein size is comparable with the nanometer-scale building blocks, these nanoparticles displayed a great effect on the electron exchange assistance between catalase and carbon

paste electrode [46]. For further investigate the catalase characteristics at the CAT / ZnO Nps/ CPE, the effect of different scan rates (50, 100, 200, 300, 400, 500 and 600 mv/s) on the catalase voltammetric behavior was studied in detail. With an increasing scan rate, the redox peak currents increased simultaneously, accompanied enlarged the peak separation. Moreover, both the cathodic and anodic peak currents increased linearly with the scan rate. The baseline subtraction procedure for the cyclic voltammograms was obtained in accordance with the method reported by Bard and Faulkner [47]. The scan rate (ν) dependence of the heights and potentials of the peaks is plotted in Figure 6(b). It can be seen that the redox peak currents increased linearly with the scan rate, the correlation coefficient was 0.9955 (ipc = -0.0141ν - 0.6386) and 0.9941 (ipa = 0.0157ν + 1.6701), respectively. This phenomenon suggested that the redox process was an adsorption-controlled and the immobilized catalase was stable. In a research, Ali Babaei et al. worked on a sensor for simultaneous determination of dopamine and morphine in biological samples using a multi-walled carbon nanotube/chitosan composite modified glassy carbon electrode, ipa(μA) = 0.1108*v* + 5.9339 (mV s^{-1}) (R^2 = 0.9908) [48].

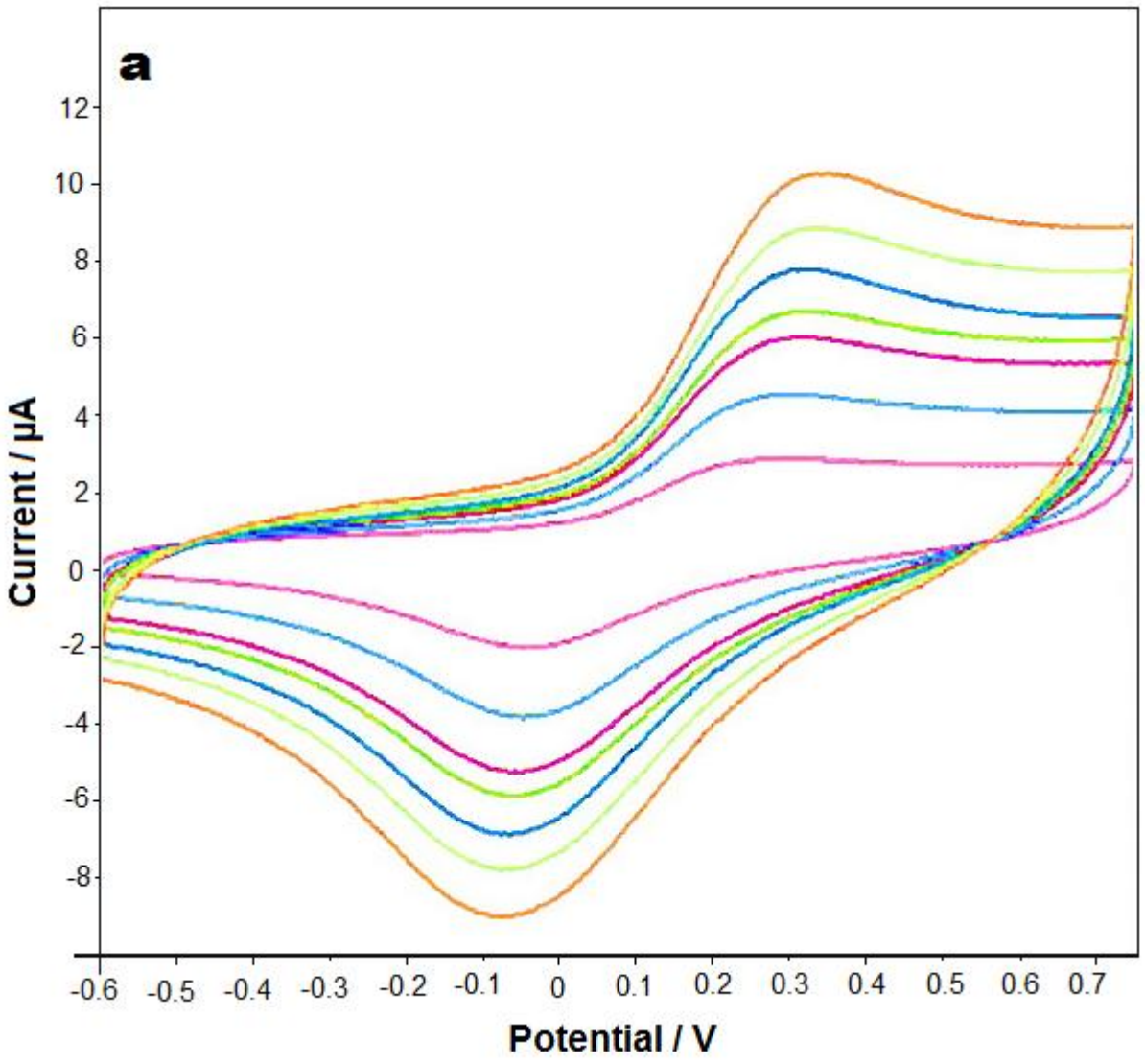

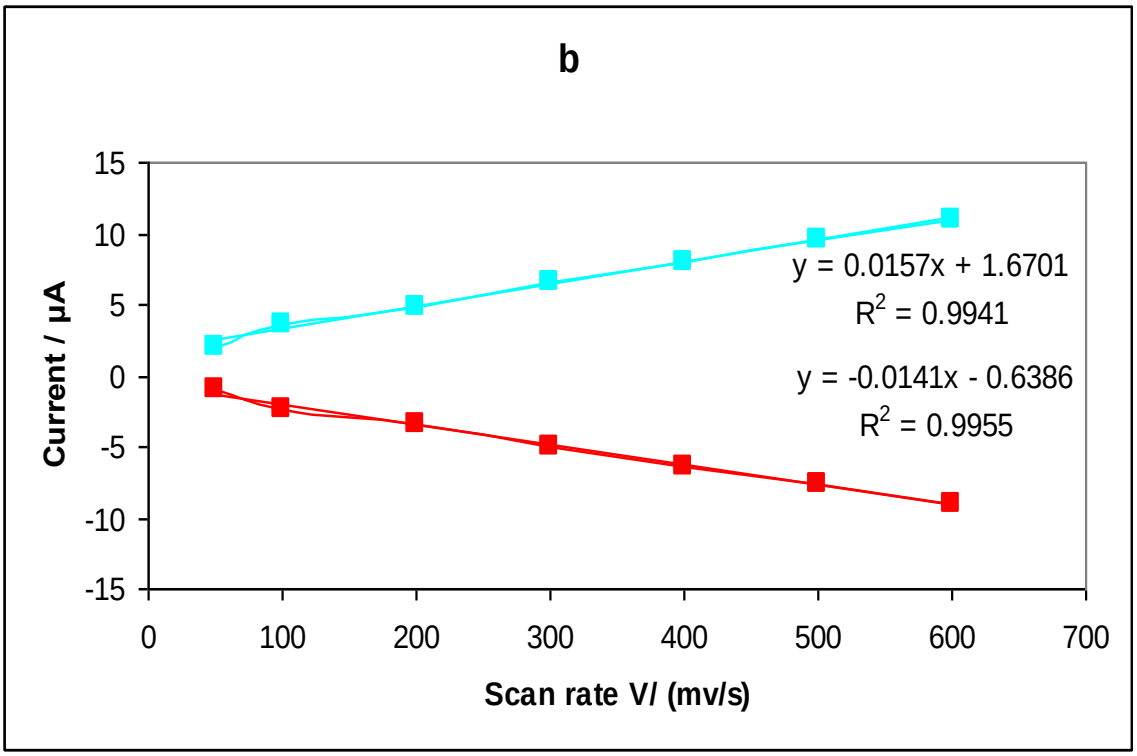

Figure 6. (a) Typical cyclic voltammograms of CAT / ZnO Nps/ CPE at different scan rates. The voltammograms (from inner to outer) designate scan rates of 50, 100, 200, 300, 400, 500 and 600 mV s^{-1}, respectively. (b) Dependence of the anodic and cathodic peak currents on the different scan rates. All the data were obtained at pH 7.0 and in 0.1M PBS.

All these results indicated that the CAT immobilized on ZnO Nps/ CPE surface controlled and quasi-reversible electrochemical reaction process. When the peak-to-peak separation (ΔE) was larger than 200 mV, the apparent heterogeneous electron transfer rate constants (ks) would be easily calculated with the help of Laviron's equations [49-50] as follows:

$$E_{p,catodic} = E^0 + \frac{RT}{\alpha F} \ln \frac{RTks}{\alpha Fv} \quad (2)$$

$$E_{p,anodic} = E^0 + \frac{RT}{(1-\alpha)F} \ln \frac{RTks}{(1-\alpha)Fv} \quad (3)$$

$$\Delta Ep = Ep,_{anodic} - Ep,_{catodic} = \frac{RT}{\alpha(1-\alpha)F} \quad (4)$$

$$[\log ks = \alpha \log(1-\alpha) + (1-\alpha)\log\alpha - \log\frac{RT}{nFv} - \frac{\alpha(1-\alpha)nF\Delta EP}{2.3\,RT}] \quad (5)$$

Where α is the electron transfer coefficient. Here, n is the number of transferred electrons at the rate of determining reaction. *R*, *T* and *F* are gas, temperature and Faraday constant, respectively (*R* = 8.314 J mol^{-1} K^{-1}, *F* = 96493 C/mol, *T* = 298 K) and ks is the apparent heterogeneous electron transfer rate constants which can be calculated according to ΔEp versus ln *v*. The value of ks was calculated to

be 2.01 s^{-1}. The ks value directly showed that CAT / ZnO Nps/ CPE complex together enhanced the electron transfer rate between CAT and carbon paste electrode.

3.5. Effect of pH on the formal potential of CAT / ZnO Nps/ CPE

Figure 7 shows the formal potential of CAT, immobilized onto the modified carbon paste electrode with ZnO nanoparticles; in PBS has a strong dependence on the pH of solution. All the changes in the peak potentials and currents with solution pH were reversible in the pH range from 3.85 to 10.1. An increase in the solution pH caused a negative shift in both cathodic and anodic peak potentials according to formal potential rates. Plot of the formal potential versus pH (from 3.85 to 10.1) showed a line with the slope of - 17 mV pH^{-1}.

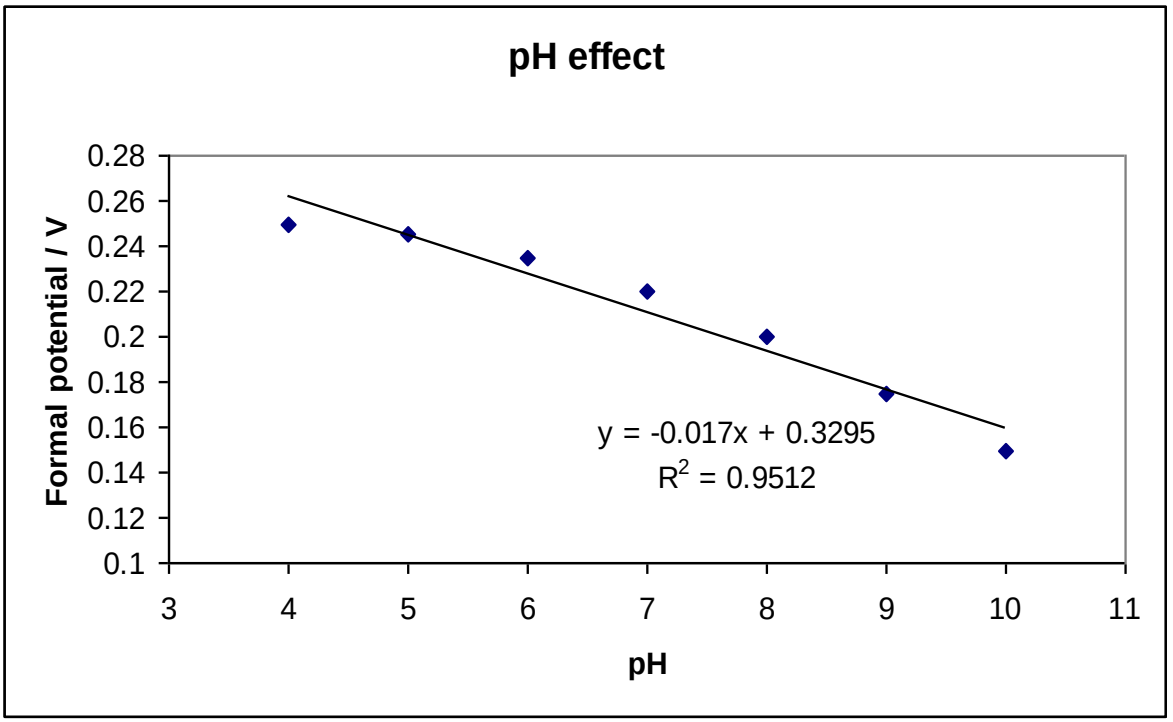

Figure 7. Effect of pH on the formal potential of CAT / ZnO Nps/ CPE

3.6. Design a dopamine biosensor with CAT / ZnO Nps/ CPE

An increase in the current or a shift in the reaction potential to more facile direction for an electrochemical reaction observed on amodified electrode surface is so called the electrocatalytic effect of the modifier [51]. Interestingly, here, both effects are observed for CAT / ZnO Nps/ CPE towards the oxidation of DA (figure 8.a&b). Figure (8 a) indicates that anodic current increases with successive addition of dopamine. Variations of the oxidation peak current of DA (ipa) as a function of the potential scan rate (v) depicted a linear behavior Upon addition of different concentrations of dopamine; this result Indicating that the charge transfer rate at the CAT / ZnO Nps/ CPE electrode

surface is controlled by the redox reaction of DA adsorbed on the surface. This behavior is used in this work to develop a method for direct determination of DA based on anodic adsorptive voltammetry. It was observed that the peak currents enhanced greatly at ZnO nanoparticles modified CPE, which provides high surface area of the ZnO nanoparticles improved the electrode contacting area of DA and its electrochemistry of reaction product, which increased. The result indicated that the electron transfer reaction was controlled by diffusion and increases in the concentrations of DA. In this research the anodic peak current of DA showed a linear relationship for different concentrations of DA (figure 8.b) in the range of 5 to 41 μM. The linear equation was expressed as ipa(μA) = 0.4226 - 0.1709 (μM) (R^2 = 0.9996) with a detection limit of 3 μM for this interval. In a research, Cheng Yin Wang et al. worked on voltammetric determination of dopamine in human serum with amphiphilic chitosan modified glassy carbon electrode and anodic peak currents were proportional to DA concentrations in the range of $6.0 \times 10^{-8} \sim 7.0 \times 10^{-6}$ M; The linear equation is ipa (μA) = 0.972 + 0.749*C* (10^{-7} M) with a correlation coefficient, R^2 = 0.998[52]. In this research, we have studied the redox electrochemistry of dopamine (DAH_2) and its oxidized form (DA); the proposed mechanisms for electrochemical behavior of dopamine and modified carbon paste electrode with CAT / ZnO Nps were shown in equations 6, 7 and 8.

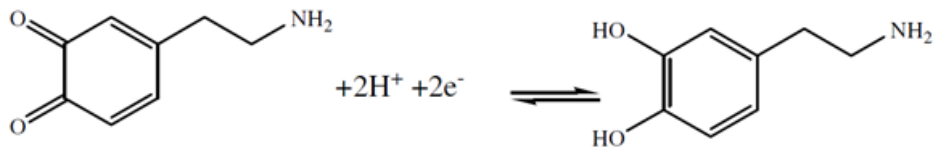

(6)

CAT(ox) + Substrate → CAT(red) + Product (7)

At electrode;

CAT(red) → CAT(ox) + e- (8)

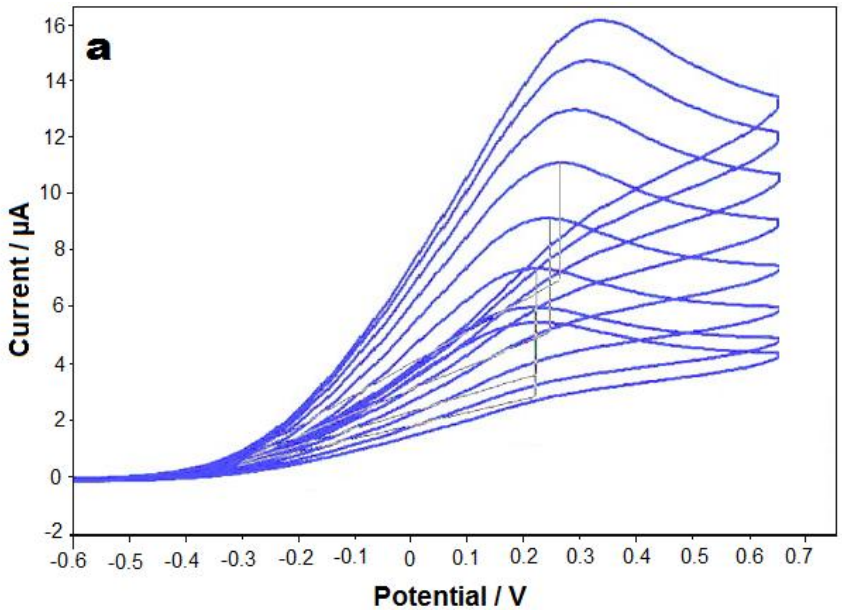

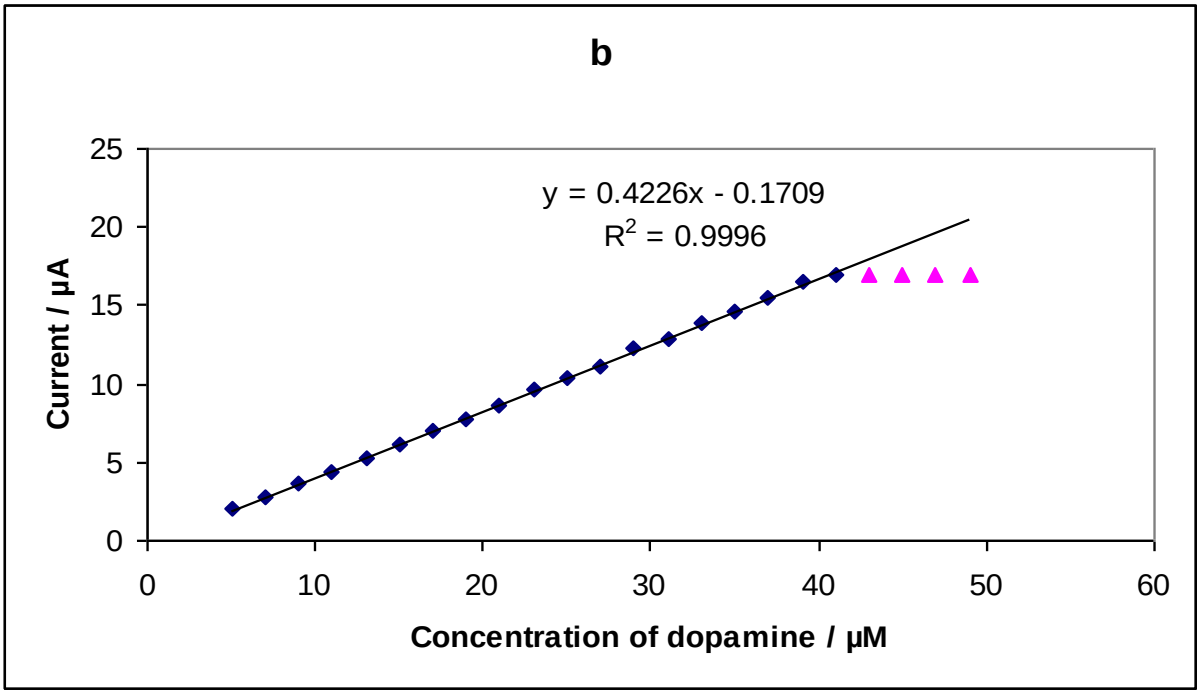

Figure 8. (a) Cyclic voltammograms obtained at an CAT / ZnO Nps/ CPE in 0.1M phosphate buffer solution (pH 7.0) for different concentrations of dopamine and (b) the relationship between anodic peak current of CAT and different concentrations of dopamine (scan rate: 100 mVs^{-1}).

3.7. Constant potential amperometry (CPA) on designed dopamine biosensor

Another electrochemical measurement carried out in this research was constant potential amperometry (CPA). CPA is a technique where a constant potential, sufficient to oxidise or reduce the analyte of interest, is applied to the electrode and the current is monitored [53].

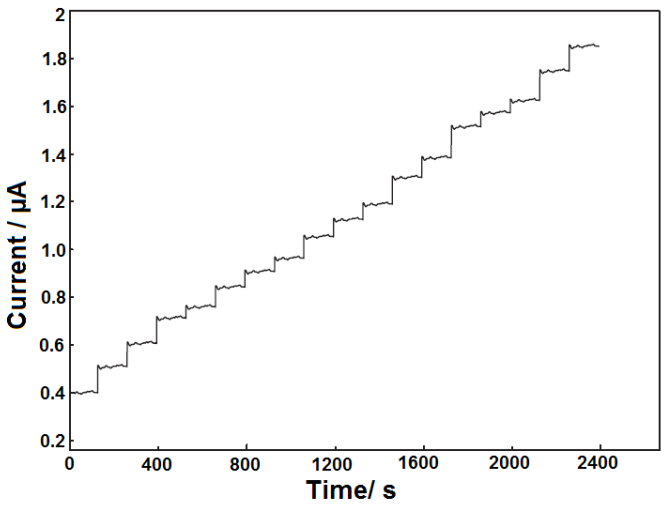

Figure 9. Amperometric responses of dopamine (each 2 µM) tested by CAT / ZnO Nps/ CPE in 0.1 M PBS (pH 7), rotating speed = 1000 rpm

CPA was used as a tool to calibrate the modified CAT / ZnO Nps/ CPE electrode to DA. This involved rotating the working electrode at high speeds until the non–faradaic current had reached a stable background level. This produces a step-wise pattern of time (s) versus current (A cm^{-2}). Figure 9 shows the amperometric responses of sequential additions of standard dopamine (each 2 μM) and tested by CAT / ZnO Nps/ CPE in 0.1 M PBS (pH 7), respectively, rotating speed = 1000 rpm. It could be found linearly dependence between amperometric current and dopamine concentration during 170－2400 s.

3.8. Effect of temperature on designed dopamine biosensor

Temperature is a key factor for most enzymatic reactions. In most cases, the activity of the enzyme increases to a special amount with increasing temperature [54]. As the temperature of the system is increased, the internal energy of the molecules in the system will increase [55]. The internal energy of the molecules may include the translational energy, vibrational energy and rotational energy of the molecules, the energy involved in chemical bonding of the molecules as well as the energy involved in nonbonding interactions. Some of this heat may be converted into chemical potential energy [56].

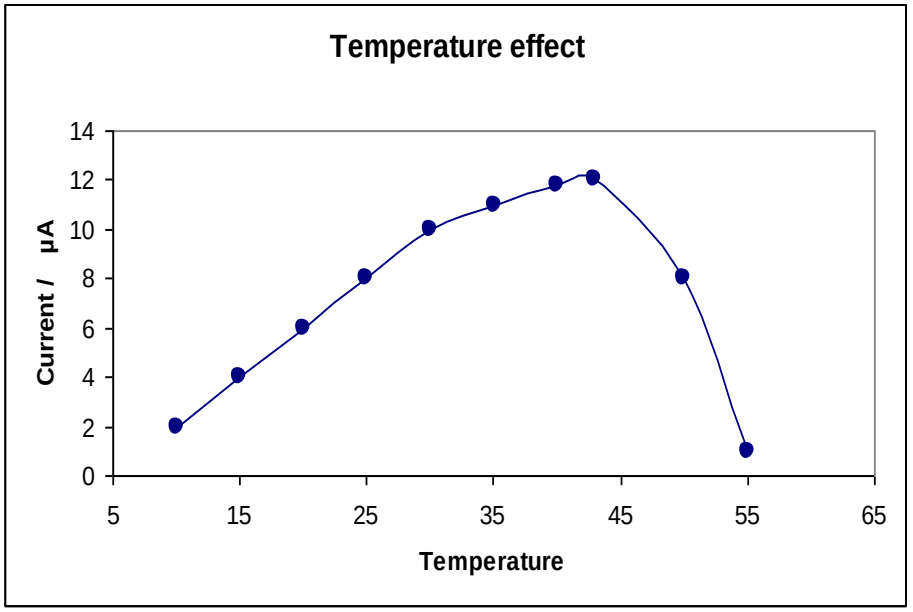

Figure 10. Effect of temperature on designed dopamine biosensor based on CAT / ZnO Nps/ CPE

If this chemical potential energy increase is great enough some of the weak bonds that determine the three dimensional shape of the active proteins many be broken [57]. This could lead to a thermal denaturation of the proteins and thus inactivate the proteins. Thus too much heat can cause the rate of an enzyme catalyzed reaction to decrease because the enzyme or substrate becomes denatured and inactive [58]. The optimum temperature for enzymes to work at is around 37ºC which is why this

temperature is body temperature. In this research, the effect of temperature on designed biosensor response was examined in the range of 10-55 ^{o}C. The results showed that the response decreased at temperatures above 42 ^{o}C, probably due to damage to the structure and denaturation of catalase enzyme. In addition, at higher temperatures, the lifetime of the biosensor was shortened; details about this experiment were shown in figure 10. Considering lifetime of sensor and operational convenience, the room temperature (25 ^{o}C) was chosen as the optimum temperature for all experiments.

3.9. Stability of designed dopamine biosensor

The stability of dopamine biosensor has been checked by carrying out experiments at the regular interval of a week and it has been found that CAT / ZnO Nps/ CPE electrode based electrochemical biosensor retains its 91% activity after 21 days. The loss in the activity of biosensor is not due to the denaturation of catalase but it is due to the poor adhesion of zinc oxide Nanoparticles on the carbon paste electrode.

4. CONCLUSION

Biosensors are very important devices for detection of biological analytes and have applications in many sciences. In this study we used of combination of biology, chemistry and nanotechnology for designing a biosensor for detect of dopamine. The anodic peak current of DA showed a linear relationship for different concentrations of DA in the range of 5 to 41 μM. The biosensor showed a good reproducibility and stability and the experiments showed excellent electro analytical activity of this biosensor for dopamine detection.

References

1. Kress-Rogers, E. Handbook of Biosensors and Electronic Noses; CRC Press Inc.: New York, 1997.
2. Wise, D.L. Bioinstrumentation and Biosensors; Marcel Dekker: New York, 1991.
3. Turner, A.P.F.; Karube, I.; Wilson, G.S. Biosensors Fundamentals and Applications; Oxford Univeristy Press: Oxford, 1987.
4. Pak SC, Penrose W, Hesketh PJ. *Biosens Bioelectron,* 16 (2001) 1.
5. Arnold, M.A.; *Anal. Chem*. 20 (1988) 149.
6. Bidan, G. *Sens. Actuators* B, 6 (1992) 45.
7. Zhao J, O'Daly JP, Henkens RW, Stonehuerner J, Crumbliss AL. *Biosens Bioelectron,* 11 (1996) 493.
8. Vo-Dinh T, Cullum BM, Stokes DL. *Sens Actuators*, B 74 (2001) 2.
9. Van Gerwen P, Laureyn W, Laureys W, Huyberechts G, Op De Beeck M, Baert K, et al. *Sens Actuators*, B 49 (1998) 73.
10. Ramsay, G. Commercial Biosensors; in the series Chemical Analysis; Winefordner, J.D., Ed.; John Wiley & Sons Inc.: New York, 1998.
11. R. S. Nicholson, *Anal. Chem*., 38 (1966) 1406.
12. Herna´ndez-Santos D, Gonza´lez-Garcı´a MB, Garcı´a AC. *Electroanalysis*, 14 (2002) 35.

13. Cui Y, Wei Q, Park H, Lieber CM. *Science*, 293 (2001) 92.
14. Zhao Y-D, Zhang W-D, Chen H, Luo Q-M, Li SFY. *Sens Actuators, B*, 87 (2002) 72.
15. Y.Sun, J.Fei, K.Wu, S.Hu, *Anal.Bioanal.Chem*. 375 (2003) 544.
16. Y.Kamitaka, S.Tsujimura, *Phys. Chem. Chem. Phys*. 9 (2007) 1793.
17. K.G.Lim and G.T .R.P almore, *Biosens. Bioelectron*. 22 (2007) 941.
18. Saeed Rezaei-Zarchi, Masoud Negahdary, *Advances in Environmental Biology*. 5(2011) 3241.
19. Allan J. Bard, *Journal of Chemical Education*, 60 (1983) 302.
20. J. Wang, M. Musameh, *Anal. Chem*. 75 (2003) 2075.
21. Y.Kamitaka, S.Tsujimura, *Phys. Chem. Chem. Phys*. 9 (2007) 1793.
22. Look D.C, *matscieng*; B.80 (2001) 383.
23. Brayner, R., R. Ferrari-Iliou, N. Brivois, S. Djediat, M. F. Benedetti, and F.Fievet. *Nano Lett*. 6(2006) 866.
24. P. Nicholls and G. R. Schonbaum In: Boyer P D, Lardy H, Myrback K, (Eds.), *The Enzymes, Vol. 8*, Academic Press, Orlando (1963).
25. M. Buleandra, G. L. Radu and I. Tanase, Roum. *Biotechnol. Lett*., 5 (2000) 423.
26. B. Zhou, J. Wang, X.Gao, Y. Tian, *Anal. Lett*., 41(2008) 1832.
27. L. Shen, N. Hu, *Biomacromolecules*, 6 (2005) 1475.
28. K.J. Huang, .D.J. Niu, X. Liu, Z.W. Wu, Y. Fan, Y.F. Chang, Y.Y. Wu, *Electrochim. Acta*, 56 (2011) 2947.
29. L. Staudenmaier, Ber. Dtsch. *Chem. Ges*., 31 (1898) 1481.
30. Sedigheh Hashemnia, Shima Khayatzadeh, Ali Akbar Moosavi-Movahedi, Hedayatollah Ghourchian, *Int. J. Electrochem. Sci*., 6 (2011) 581.
31. P. Damier, E. C. Hirsch, Y. Agid and A. M. Graybiel, Brain, 122 (1999) 1437
32. C. Martin, *Chem. Br*., 34 (1998) 40
33. A. Heinz, H. Przuntek, G. Winterer and A. Pietzcker, *Nervenarzt*, 66 (1995) 662
34. J. R. Cooper, F. E. Bloom and R. H. Roth, *The Biochemical Basis of Neuropharmacology*; Oxford University Press, NewYork, 1986
35. B. Jill Venton, R. Mark Wightman, *Anal. Chem*. 75 (2003) 414A-421A.
36. M.D. Hawley, S.V. Tatawawadi, S. Pierkarski, R. N. Adams, *J. Am. Chem. Soc*., 89 (1967) 447.
37. Montague P.R., Dayan P., Sejnowski T.J., *J Neurosci*, 16(1996) 1936.
38. Tzschentke T.M., *Prog Neurobiol*, 63(2001)241.
39. Skoog, et al. Principles of Instrumental Analysis. 6th ed. Thomson Brooks/Cole. (2007) 349.
40. Skoog, et al. Principles of Instrumental Analysis. 6th ed. Thomson Brooks/Cole. (2007), 169.
41. P. Harrison, *Quantum wells, wires and dots*, Wiley, 2005.
42. S. Rezaei-Zarchi, A. A. Saboury, J. *Appl. Electrochem*., 37 (2007) 1021.
43. Lee SP, Lee SJ, Lim BS, Ahn SJ, *Angle Orthod*., 79 (2009) 353.
44. Reza Karimi Shervedani and Hossein Ali Alinajafi-Najafabadi, *International Journal of Electrochemistry,* (2011), doi:10.4061/2011/603135
45. J.G.Manjunatha, B.E. Kumara Swamy, G.P.Mamatha, Umesh Chandra, E.Niranjana, and B.S.Sherigara, *Int. J. Electrochem. Sci.*, 4 (2009) 187.
46. K.Wu, J.Fei, W.Bai, S.Hu, *Anal.Bioanal.Chem*.376 (2003) 205.
47. A.J. Bard, L.R. Faulkner, Electrochemical Methods, second. ed., Fundamentals and Applications, Wiley, NY, (2001) 241.
48. Ali Babaei, M. Babazadeh, H. R. Momeni, *Int. J. Electrochem. Sci*., 6 (2011) 1382.
49. E. Laviron, *J. Electroanal. Chem*., 101 (1979) 19.
50. E. Laviron, *J. Electroanal. Chem*., 100 (1979) 263.
51. M. Senda and P. Delahay, *Journal of Physical Chemistry*, 65(1961)1580.
52. Cheng Yin Wang, Zhi Xian Wang, Ai Ping Zhu and Xiao Ya Hu, *Sensors*, 6 (2006) 1523.
53. J. P. Lowry and R. D. O'Neill, C. A. Grimes, E. C. Dicky, and M. V. Pishko, *American Scientific Publishers, Encyclopedia of Sensors*, 10(2006) 1.

54. Martinek, R, *J. Am. Med. Tech*., 31(1969) 162.
55. Bennett, T. P., and Frieden, E.: Modern Topics in Biochemistry, Macmillan, London (1969).
56. Holum, J.: *Elements of General and Biological Chemistry*, 2nd ed., 377, Wiley, NY (1968).
57. Harrow, B., and Mazur, A.: *Textbook of Biochemistry,* 109, Saunders, Philadelphia (1958).
58. Pfeiffer, J.: *Enzymes, the Physics and Chemistry of Life*, Simon and Schuster, NY (1954).

© 2012 by ESG (www.electrochemsci.org)